

# Mono- and dinuclear (*o*-thioetherphenolato)-copper(II) complexes. Structural models for galactose oxidase

Tobias Kruse, Thomas Weyhermüller, Karl Wieghardt \*

Max-Planck-Institut für Strahlenchemie, Stiftstrasse 34-36, D-45470 Mülheim an der Ruhr, Germany

Received 29 June 2001; accepted 14 August 2001

Dedicated to Professor A.G. Sykes

## Abstract

Three new *o*-thioetherphenol ligands have been synthesized: 1,2-bis(3,5-di-*tert*-butyl-2-hydroxyphenylsulfanyl)ethane (H<sub>2</sub>bse), 1,2-bis(3,5-di-*tert*-butyl-2-hydroxyphenylsulfanyl)benzene (H<sub>2</sub>bsb), and 4,6-di-*tert*-butyl-2-phenylsulfanylphenol (Hpsp). Their complexes with copper(II) were prepared and investigated by UV–Vis-, EPR-spectroscopy; their electro- and magnetochemistry have also been studied: [Cu<sup>II</sup>(psp)<sub>2</sub>] (1), [Cu<sup>II</sup>(bse)<sub>2</sub>] (2), [Cu<sup>II</sup>(bsb)<sub>2</sub>] (3), [Cu<sup>II</sup>(bsb)(py)<sub>2</sub>] (4). The crystal structures of the ligands H<sub>2</sub>bse, H<sub>2</sub>bsb, Hpsp and of the complexes 1, 2, 3, 4 have been determined by X-ray crystallography. © 2002 Elsevier Science B.V. All rights reserved.

**Keywords:** *o*-Thioetherphenols; Copper complexes; Galactose oxidase models; Magnetochemistry

## 1. Introduction

In the resting state of the enzyme *galactose oxidase*, a single Cu(II) ion is coordinated in a distorted square-based pyramidal fashion to two histidine N-donor atoms (His 496, His 581), two tyrosinato oxygen atoms (Tyr 495, Tyr 272) and a labile water molecule [1]. Tyr 272 exhibits a peculiar post-translational modification. It forms in the *ortho* position, a thioether linkage to a neighboring cystein residue (Cys 228). The thioether sulfur is only weakly, if at all, coordinated to the Cu(II) ion (Cu⋯S 3.58 Å). In a number of model studies, the role of this *o*-thioetherphenolato moiety has been investigated [2] since this is the locus where one-electron oxidation generating the active form of the enzyme, namely a coordinated Cu<sup>II</sup>-tyrosyl radical moiety, occurs [3].

We have previously shown [4] that it is possible to synthesize a functional model for the aerobic oxidation of alcohols by using a (2,2'-thio-bis(2,4-di-*tert*-butylphenolato)copper(II) complex, which in its dimeric

form is readily oxidized by dioxygen to produce reactive (phenoxy)copper(II) species.

Here we report an attempt to systematically vary the structural features and thereby the coordinating ability of similar *o*-thioetherphenol ligands. To this end, we have synthesized the ligands and complexes shown in Scheme 1.

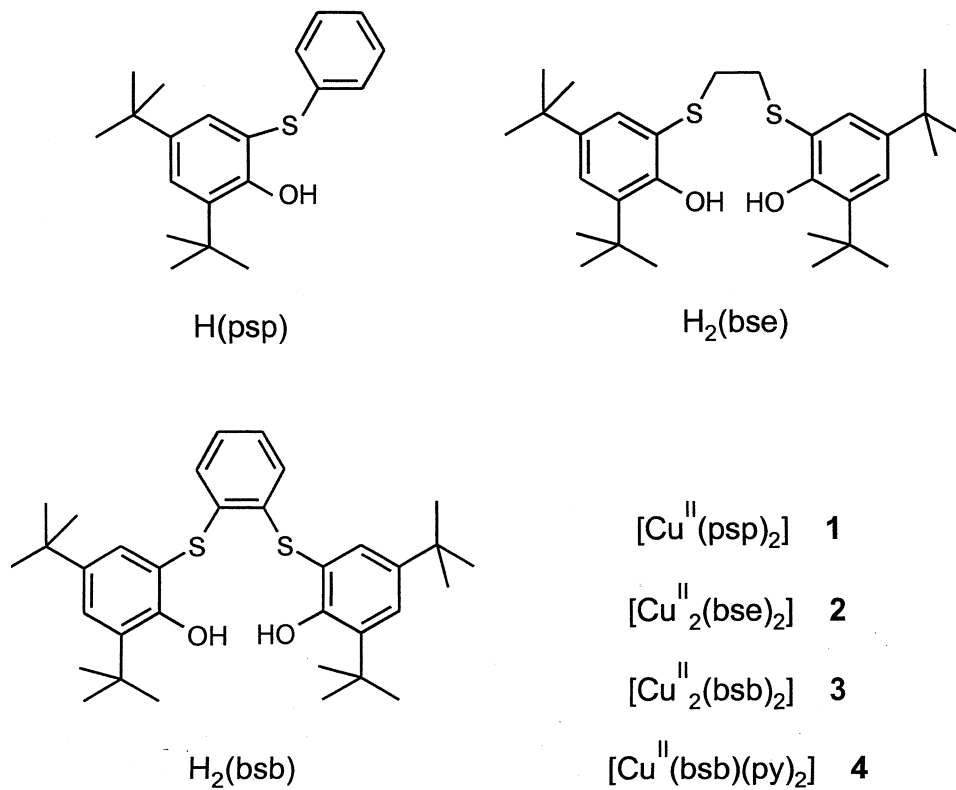
## 2. Results and discussion

### 2.1. Syntheses

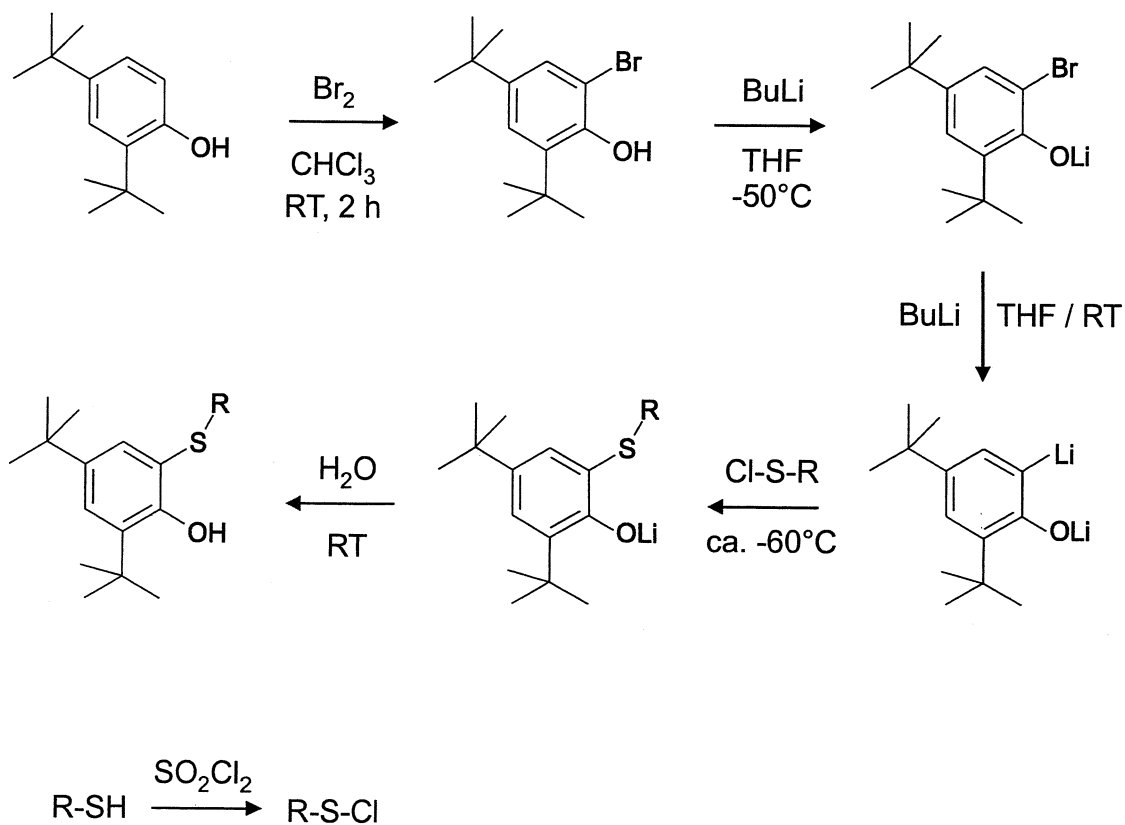
The three new *o*-thiophenol ligands were synthesized following the general route displayed in Scheme 2. 2,4-Di-*tert*-butylphenol was brominated in chloroform at ambient temperature affording 2-bromo-4,6-di-*tert*-butylphenol in excellent yields. This compound was lithiated in two successive 1 equiv. steps in tetrahydrofuran at –50 °C by using commercially available *n*-butyllithium in *n*-hexane solutions. After addition of the second equivalent, the solution was allowed to slowly warm-up to 20 °C. The success of this preparation critically depends on the rigorous absence of water and on the purity of reagents and solvents. Excess

\* Corresponding author. Tel.: +49-208-306 3609/10; fax: +49-208-306 3952.

E-mail address: wieghardt@mpi-muelheim.mpg.de (K. Wieghardt).



Scheme 1.



Scheme 2.

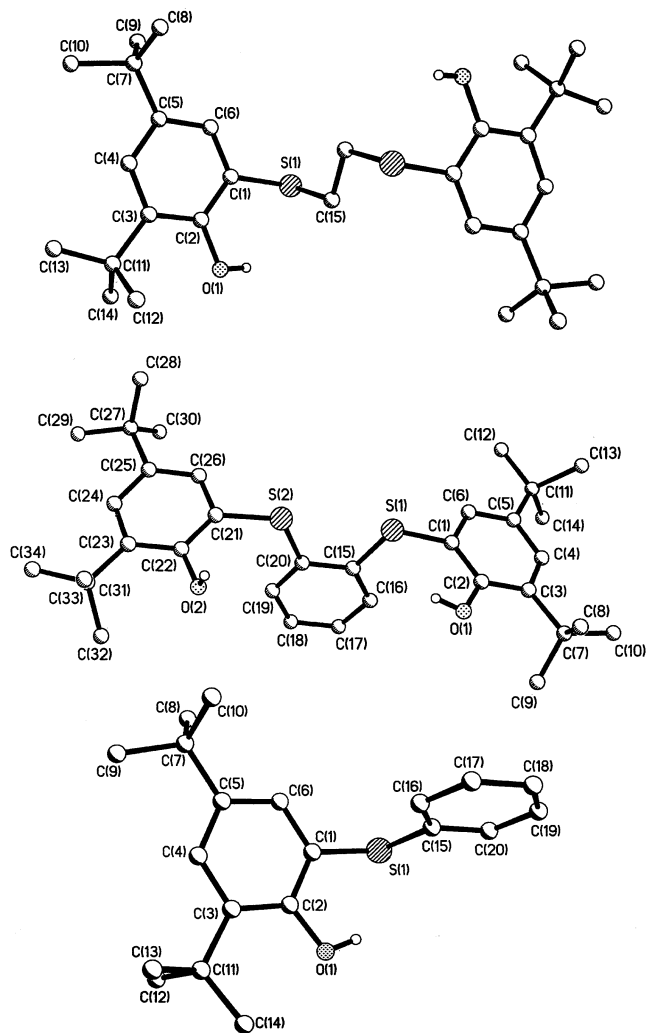
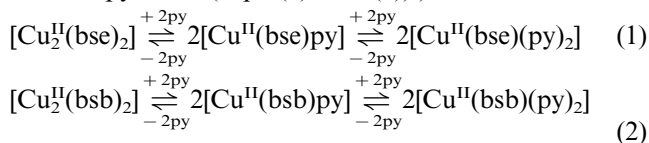


Fig. 1. Molecular structures of  $H_2bse$  (top),  $H_2bsb$  (middle), and  $Hpsp$  (bottom).

*n*-butyllithium must be avoided. To these solutions was added exactly 1 or 1.5 equiv. of the corresponding sulfenyl- or disulfenyl chloride yielding the *o*-thiophenol ligands and  $LiCl$ . The sulfenyl chlorides were prepared by the reaction of the starting thiol with  $SO_2Cl_2$  in  $CH_2Cl_2$  solution at temperatures in the range  $-30$  to  $0$  °C [5]. Effervescence of  $HCl$  is observed until 1.5 equiv. of  $SO_2Cl_2$  has been added. In the case of a dithiol starting material, the formation of insoluble polymers containing disulfide bridges occurred. After addition of the second half equivalent of  $SO_2Cl_2$  these redissolved with formation of the desired disulfenyl dichlorides.

The synthesis of the copper(II) complexes containing monoanionic  $(psp)^{1-}$ , or dianionic  $(bse)^{2-}$  and  $(bsb)^{2-}$  ligands is straightforward. Thus, the reaction of 2 equiv. of  $Hpsp$  with 1 equiv. of  $Cu^I Cl$  and 2 equiv. of the base triethylamine in the presence of air in methanol yields brown crystals of  $[Cu^{II}(psp)_2]$  (**1**).

The green–brown complexes  $[Cu_2^{II}(bse)_2]$  (**2**) and  $[Cu_2^{II}(bsb)_2]$  (**3**) were obtained from the reaction of  $H_2bse$ , or  $H_2bsb$  and  $CuCl$  (1:1) in THF in the presence of air upon addition of 2 equiv. of  $NEt_3$ . Both **2** and **3** are bis( $\mu$ -phenolato)dicopper(II) species. It is well established chemistry of such dinuclear species [2c–e] that they can form penta- and even hexadentate mononuclear complexes via addition of coordinating ligands such as pyridine (Eqs. (1) and (2)).



Mononuclear  $[Cu(bsb)(py)_2]$  (**4**) has been isolated as crystalline material and its crystal structure has been determined (see below).

Fig. 4 displays the electronic spectra of **2** and **3** in  $CH_2Cl_2$  solution. Both display an intense absorption maximum at 450 nm ( $\epsilon = 3.3 \times 10^3$  l mol $^{-1}$  cm $^{-1}$ ) for **2** and at 470 ( $2.3 \times 10^3$ ) for **3**. A second maximum which is assigned to a predominantly d–d transition is observed at 645 nm ( $\epsilon = 1.45 \times 10^3$  l mol $^{-1}$  cm $^{-1}$ ) for **2** and at 620 (630) for **3**. Upon addition of 2 equiv./dimer of pyridine, the spectra change dramatically; a color change from brown to violet is observed. Both absorption maxima in the visible of **2** and **3** are less intense and they are shifted to longer wavelengths:  $[Cu^{II}(bse)py]$ :  $\lambda_{max} = 464$  nm ( $\epsilon = 1.2 \times 10^3$  l mol $^{-1}$  cm $^{-1}$ ) and 769 (680);  $[Cu^{II}(bsb)py]$ : 517 (580) and 743 (250). Upon addition of a further 2–4 equiv. of pyridine to these solutions, the spectra do not change significantly. Thus, the spectra of the hexacoordinate species resemble closely those of the five-coordinate intermediates.

## 2.2. Crystal structures

The molecular structures of the ligands  $H_2bse$ ,  $H_2bsb$ ,  $Hpsp$  have been determined by X-ray crystallography at cryogenic temperatures (100(2) K). Fig. 1 shows the structures of these organic molecules. Bond distances and angles are available in the supplementary material; they do not show any unusual features. The molecular structures of complexes **1–4** have also been determined. Crystallographic data of all structure determinations are summarized in Table 1; Table 2 gives selected bond distances and angles of the complexes. Fig. 2 displays the structures of the neutral mononuclear species in crystals of **1** and **4** whereas Fig. 3 shows those of the dinuclear complexes in crystals of **2** and **3**.

The copper(II) ion in **1** is *O,S*-coordinated to two bidentate  $(psp)^{1-}$  monoanions; it is in a nearly planar  $O_2S_2$ -coordination sphere with a slight distortion toward a tetrahedron. The two  $(psp)^{1-}$  ligands are in *trans*-position relative to each other. The average Cu–O

and Cu–S distances are short at 1.848(2) and 2.345(1) Å, respectively. In the solid state, two mononuclear [Cu(psp)<sub>2</sub>] entities form a dimer via two very weak Cu–S⋯Cu\* interactions. The S1⋯Cu\* distance is 3.131(1) Å and the ‘intramolecular’ Cu⋯Cu\* distance is 4.371(1) Å.

In contrast, the Cu(II) ion in **4** is six-coordinate in a S<sub>2</sub>O<sub>2</sub>N<sub>2</sub> donor environment composed of two thioether S-donors in *cis*-position relative to each other and two pyridine N-donors also in *cis*-position, whereas the two phenolato O-donor atoms are *trans* relative to each other. The two Cu–S and Cu–N bonds are not equidistant whereas the two Cu–O bonds at an av. 1.930(3) Å are equivalent within experimental error. The N1–Cu–S2 axis clearly defines a Jahn Teller axis of a tetragonally elongated distorted O<sub>2</sub>N<sub>2</sub>S<sub>2</sub>Cu octahedron (static Jahn Teller distortion).

As shown in Fig. 3 crystals of **2** and **3** contain the centrosymmetric dinuclear species [Cu<sub>2</sub><sup>II</sup>(bse)<sub>2</sub>] and [Cu<sub>2</sub><sup>II</sup>(bsb)<sub>2</sub>], respectively. The dianionic ligands (bse)<sup>2-</sup> and (bsb)<sup>2-</sup> are each coordinated to one of the Cu<sup>II</sup> ions via two Cu-thioether and a terminal Cu-phenolato bond. In addition, the second phenolato group of both

ligands forms a μ-phenolato bridge to the respective second Cu<sup>II</sup> ion. Thus, both Cu<sup>II</sup> ions are five-coordinate in a distorted square-based pyramidal environment. One thioether sulfur donor is always in an apical position whereas the second occupies a basal coordination site. The Cu⋯Cu distance in **2** is at 2.814(1) Å but slightly longer at 2.904(2) Å in **3** and, concomitantly, the Cu–O–Cu angle at 90.8(1)° in **2** is smaller by 5.3° than in **3**.

### 2.3. Magnetic susceptibility and EPR spectroscopic data

The temperature dependent magnetic susceptibilities of complexes have been measured in the range 2–298 K by using a SQUID magnetometer and an external magnetic field of 1 T. The raw magnetic susceptibility data were corrected for underlying diamagnetism by the use of tabulated Pascal’s constants (Fig. 4).

In the solid state the two didentate ligands of **1** are in *trans*-position relative to each other and two such entities form a weakly S-bridged dimer [Cu<sup>II</sup>(psp)<sub>2</sub>]<sub>2</sub> as shown in Fig. 2 (top). In excellent agreement with this

Table 1  
Crystallographic data for H<sub>2</sub>(bse), H<sub>2</sub>(bsb), and H(psp), **1**, **2**, **3**, and **4**

	H <sub>2</sub> (bse)	H <sub>2</sub> (bsb)	H(psp)	<b>1</b>	<b>2</b>	<b>3</b>	<b>4</b>
Chemical formula	C <sub>30</sub> H <sub>46</sub> O <sub>2</sub> S <sub>2</sub>	C <sub>34</sub> H <sub>46</sub> O <sub>2</sub> S <sub>2</sub>	C <sub>20</sub> H <sub>26</sub> OS	C <sub>40</sub> H <sub>50</sub> CuO <sub>2</sub> S <sub>2</sub>	C <sub>60</sub> H <sub>88</sub> Cu <sub>2</sub> O <sub>4</sub> S <sub>4</sub>	C <sub>68</sub> H <sub>88</sub> Cu <sub>2</sub> O <sub>4</sub> S <sub>4</sub>	C <sub>44</sub> H <sub>54</sub> CuN <sub>2</sub> O <sub>2</sub> S <sub>2</sub>
Formula weight	502.79	550.83	314.47	690.46	1128.62	1224.70	770.55
Crystal size (mm)	0.52 × 0.42 × 0.12	0.3 × 0.2 × 0.2	0.4 × 0.4 × 0.3	0.28 × 0.18 × 0.06	0.26 × 0.24 × 0.06	0.60 × 0.07 × 0.06	0.14 × 0.11 × 0.07
Space group	<i>P</i> 2 <sub>1</sub> / <i>c</i>	<i>P</i> 2 <sub>1</sub> / <i>n</i>	<i>P</i> 2 <sub>1</sub> / <i>c</i>	<i>C</i> 2/ <i>c</i>	<i>C</i> 2/ <i>c</i>	<i>P</i> 2 <sub>1</sub> / <i>c</i>	<i>P</i> 2 <sub>1</sub> / <i>n</i>
<i>a</i> (Å)	16.148(3)	16.175(3)	8.619(2)	29.729(4)	19.145(2)	12.384(3)	9.804(2)
<i>b</i> (Å)	10.006(2)	12.580(3)	12.585(3)	13.875(2)	10.486(1)	15.218(3)	18.357(4)
<i>c</i> (Å)	9.060(2)	17.102(3)	17.367(4)	21.983(3)	31.250(3)	17.624(4)	22.535(5)
β (°)	98.44(3)	112.88(3)	102.55(3)	125.12(2)	105.83(2)	94.06(3)	90.76(2)
<i>V</i> (Å <sup>3</sup> )	1448.0(5)	3206.1(11)	1838.8(6)	7417(2)	6035.8(10)	3313.1(13)	4055(2)
<i>Z</i>	2	4	4	8	4	2	4
<i>T</i> (K)	100(2)	100(2)	100(2)	100(2)	100(2)	100(2)	100(2)
ρ calcd (g cm <sup>-3</sup> )	1.153	1.141	1.136	1.237	1.242	1.228	1.262
Number of data/2θ <sub>max</sub> (°)	10 771/50.00	12 814/49.98	17 296/60.00	54 186/55.00	20 023/46.52	14 140/45.00	13 568/45.00
Number of unique data	2524	5182	5258	8502	4305	4286	5264
Number of parameters/resstraints	178/0	436/0	238/15	418/0	328/0	346/16	460/0
μ (Mo Kα) (cm <sup>-1</sup> )	2.08	1.93	1.76	7.33	8.86	8.12	6.79
<i>R</i> <sub>1</sub> <sup>a</sup>	0.0649	0.0451	0.0900	0.0529	0.0450	0.0795	0.0531
<i>wR</i> <sub>2</sub> <sup>b</sup> (all data)	0.1683	0.1105	0.2375	0.1635	0.0865	0.2073	0.1074
Goodness-of-fit <sup>c</sup>	1.094	0.930	1.099	1.049	0.971	1.072	0.963

<sup>a</sup> Observation criterion:  $I > 2\sigma(I)$ .  $R_1 = \sum ||F_o| - |F_c|| / \sum |F_o|$ .

<sup>b</sup>  $wR_2 = [\sum w(F_o^2 - F_c^2)^2] / \sum w(F_o^2)^2]^{1/2}$  where  $w = 1/\sigma^2(F_o^2) + (aP)^2 + bP$ ,  $P = (F_o^2 + 2F_c^2)/3$ .

<sup>c</sup>  $\text{Goof} = [\sum w(F_o^2 - F_c^2)^2 / (n - p)]^{1/2}$  where  $n$  = number of reflections and  $p$  = number of parameters.

Table 2  
Selected bond distances (Å) and angles (°)

Complex 1			
Cu–O1	1.846(2)	S1–C6	1.773(4)
Cu–O2	1.851(2)	S1–C7	1.789(3)
Cu–S1	2.351(1)	S2–C27	1.777(3)
Cu–S2	2.340(1)	S2–C26	1.779(3)
		O1–C1	1.343(4)
		O2–C21	1.335(4)
O1–Cu–O2	165.4(1)	O1–Cu–S1	87.5(1)
O1–Cu–S2	95.3(1)	O2–Cu–S1	94.8(1)
O2–Cu–S2	87.2(7)	S2–Cu–S1	161.05(3)
Complex 2			
Cu–O2	1.861(3)	S1–C1	1.778(4)
Cu–O1	1.927(3)	S1–C29	1.829(4)
Cu–O1*	2.023(3)	O1–C2	1.351(4)
Cu–S2	2.373(1)	S2–C15	1.778(4)
Cu–S1	2.622(1)	S2–C30	1.818(4)
		O2–C16	1.340(4)
Cu...Cu*	2.814(1)	Cu–O1–Cu*	90.8(1)
Complex 3			
Cu–O1	1.877(5)	S1–C6	1.774(8)
Cu–O2	1.943(5)	S1–C7	1.815(8)
Cu–O2*	1.961(5)	O1–C1	1.325(9)
Cu–S1	2.308(2)	S2–C12	1.761(9)
Cu–S2	2.766(2)	S2–C13	1.781(8)
		O2–C14	1.371(8)
Cu...Cu*	2.904(2)	Cu–O2–Cu*	96.1(2)
Complex 4			
Cu–O1	1.929(3)	S1–C2	1.777(5)
Cu–O2	1.932(3)	S1–C15	1.796(5)
Cu–N2	2.067(4)	S2–C21	1.793(4)
Cu–N1	2.394(4)	S2–C20	1.794(5)
Cu–S1	2.422(2)	O1–C1	1.334(5)
Cu–S2	2.696(2)	O2–C22	1.323(5)

The asterisk denotes atoms, which are related by a crystallographic inversion center in a given molecule.

structure the temperature dependence of the magnetic moment of **1** displays a very weak, intramolecular ferromagnetic coupling. Fig. 5 displays the temperature dependence of the magnetic moment of **1** calculated per dimer. By using the spin Hamiltonian Eq. (3), an excellent fit of the data was obtained:  $g_1 = g_2 = 2.07$ ,  $J = +0.5 \text{ cm}^{-1}$  and a temperature-independent magnetic susceptibility, ( $\chi_{\text{TIP}}$ ), of  $51 \times 10^{-6} \text{ cm}^{-3} \text{ mol}^{-1}$  per dimer.

$$H = -2JS_1S_2 + g\mu_B\mathbf{S}\mathbf{B} \quad S_1 = S_2 = 1/2 \quad (3)$$

The electronic spectrum of **1** in  $\text{CH}_2\text{Cl}_2$  solution displays absorption maxima at  $\lambda = 245 \text{ nm}$  ( $\epsilon = 4.0 \times 10^4 \text{ l mol}^{-1} \text{ cm}^{-1}$ ), 290 ( $1.7 \times 10^4$ ), 320 ( $1.25 \times 10^4$ ), 360 ( $0.5 \times 10^4$ ), 440 ( $0.3 \times 10^4$ ), 520 (broad tail).

Fig. 6 shows the temperature dependence of the magnetic moment/dimer of **2** (top) and **3** (bottom). Clearly, in both cases a relatively strong intramolecular ferromagnetic coupling prevails. Both data sets were satisfactorily fitted to the Hamiltonian Eq. (3). The

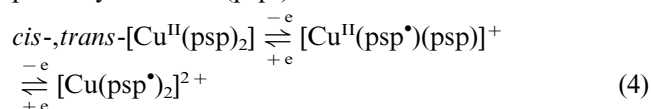
following parameters were established: **2**:  $g_1 = g_2 = 2.0$ ;  $J = +36.5 \text{ cm}^{-1}$ ,  $\chi_{\text{TIP}} = 142 \times 10^{-6} \text{ cm}^{-3} \text{ mol}^{-1}$ ; **3**:  $g_1 = g_2 = 2.1$ ;  $J = +58.7 \text{ cm}^{-1}$ ,  $\chi_{\text{TIP}} = 50 \times 10^{-6} \text{ cm}^{-3} \text{ mol}^{-1}$ . These data are in excellent agreement with published magneto-structural correlations for bis( $\mu$ -phenolato)dicopper complexes [6]. According to these analyses, the main structural parameter responsible for ferromagnetic exchange coupling is the Cu–O–Cu angle. At  $90^\circ$  the magnetic orbitals are orthogonal and maximum stabilization of the  $S = 1$  ground state is achieved. In **2** this Cu–O–Cu angle is  $90.8(1)$  and  $96.1(2)^\circ$  in **3**, and, consequently, the coupling is ferromagnetic in both cases.

The X-band EPR spectra of mononuclear **4** and dinuclear **3** in frozen  $\text{CH}_2\text{Cl}_2$  solutions measured at 10 K are shown in Fig. 7. The spectrum of **4** confirms the  $S = 1/2$  and that of **3** the  $S = 1$  ground state, respectively. The spectrum of **4** is most probably that of the square-based pyramidal species  $[\text{Cu}^{\text{II}}(\text{bsb})\text{py}]$ ; it displays an axial signal with Cu hyperfine coupling. A simulation of this spectrum gives the parameters:  $g_x = 2.06$ ,  $g_y = 2.11$ ,  $g_z = 2.22$  ( $g_{\text{iso}} = 2.13$ ),  $A_x = A_y = 0$  and  $A_z(\text{Cu}) = 15 \text{ mT}$  with line widths  $W_x = 19$ ,  $W_y = 23$ ,  $W_z = 10 \text{ mT}$ . This spectrum is in excellent agreement with those reported for similar mononuclear complexes [7].

In contrast, the rhombic signal of **3** confirms the triplet ground state of this dinuclear species. From a satisfactory simulation for an  $S = 1$  system, the following parameters were obtained:  $g_x = 2.15$ ,  $g_y = 2.107$ ,  $g_z = 2.02$  ( $g_{\text{iso}} = 2.09$ ),  $A_x(\text{Cu}) = 12$ ,  $A_y(\text{Cu}) = 0$ ,  $A_z = 2.5 \text{ mT}$ ;  $D = -0.006 \text{ cm}^{-1}$  and  $E = 0.002 \text{ cm}^{-1}$  ( $E/D = 1/3$ ).

#### 2.4. Electrochemistry

The electrochemistry of complexes has been investigated by square-wave (swv) and cyclic voltammetry (cv) on  $\text{CH}_2\text{Cl}_2$  solutions containing 0.10 M  $[(n\text{-bu})_4\text{N}]\text{PF}_6$  as supporting electrolyte at  $20^\circ\text{C}$ ; ferrocene was added as internal standard. The cv of **1** displays four irreversible, ligand-centered oxidations at  $E_p^{\text{ox}} = 0.50, 0.57, 0.80, \text{ and } 0.95 \text{ V}$  versus ferrocenium/ferrocene ( $\text{Fc}^+/\text{Fc}$ ) at  $20^\circ\text{C}$  and  $100 \text{ mV s}^{-1}$  scan rate. Two of these oxidations occur at very similar potentials, respectively. We interpret the observation of four oxidations as follows. In solution, a dynamic equilibrium of the *cis*- and *trans*- $[\text{Cu}(\text{psp})_2]$  forms exist. This has been proven for the Pd and Pt analogs and will be reported elsewhere [8]. Each of the coordinated *o*-thioetherphenolato(1–) ligands can then undergo a ligand-centered, one-electron oxidation yielding neutral, coordinated phenoxyl radicals ( $\text{psp}^\bullet$ )<sup>0</sup>.



These radical complexes are not stable on the time scale of a swv.

Complex **2** displays two irreversible one-electron oxidations at 0.52 and 0.71 versus  $\text{Fc}^+/\text{Fc}$  at 20 °C and 100  $\text{mV s}^{-1}$  scan rate which correspond to the generation of one and two coordinated phenoxyl radicals which are also not stable on the time scale of a swv. Similarly, complex **3** exhibits two irreversible one-electron oxidations at 0.62 and 0.99 V versus  $\text{Fc}^+/\text{Fc}$  at 20 °C and 100  $\text{mV s}^{-1}$  scan rate.

These experiments show that the *o*-thioetherphenolates can be oxidized but the oxidized species are very unstable and do not allow further spectroscopic characterizations.

### 3. Experimental

#### 3.1. Syntheses of ligands and complexes

##### 3.1.1. 1,2-Bis(3,5-di-*tert*-butyl-2-hydroxyphenyl-sulfanyl)ethane ( $H_2bse$ )

To a solution of 2-bromo-4,6-di-*tert*-butylphenol (5.71 g; 20 mmol) in dry diethylether (25 ml) a solution of 1.6 M *n*-butyllithium in *n*-hexane (25 ml) was added at –50 °C. The immediately formed precipitate redissolved upon increasing the temperature to 20 °C. The pale yellow solution was stirred for 30 min. After cooling to –65 °C, a solution of ethane-1,2-disulfenylchloride (1.63 g; 10 mmol) in dry diethylether

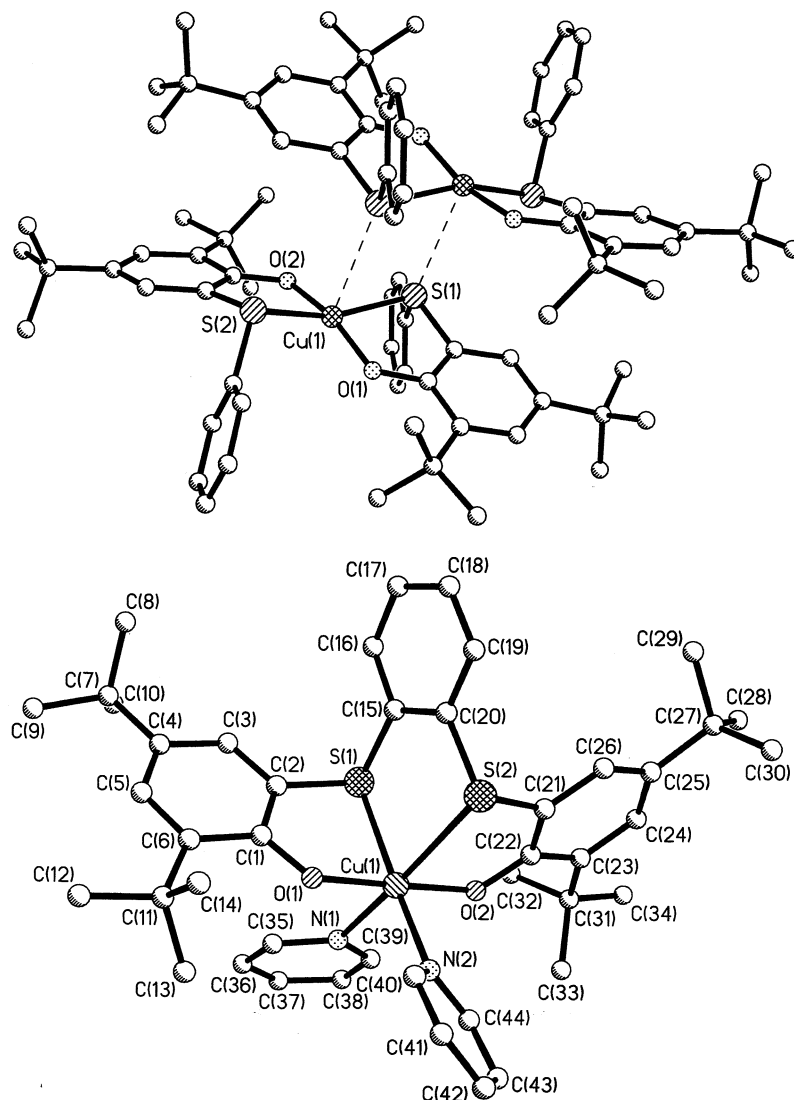


Fig. 2. Molecular structures of the neutral mononuclear complexes in crystals of **1** (top) and **4** (bottom).

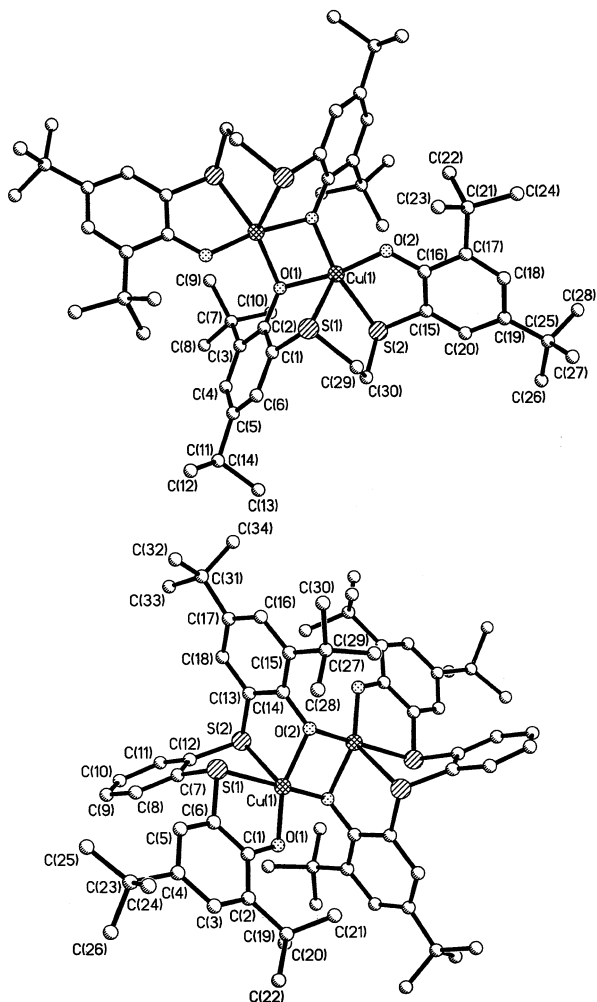


Fig. 3. Molecular structures of the dinuclear species in crystals of **2** (top) and **3** (bottom).

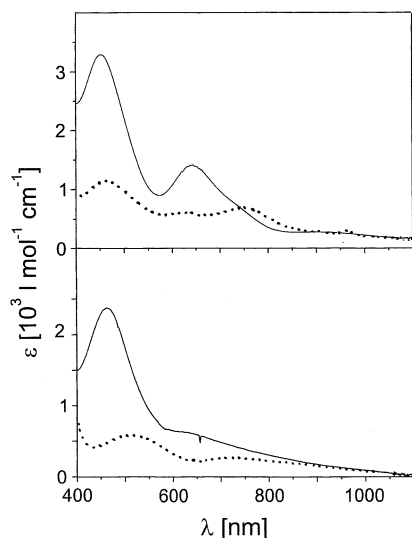


Fig. 4. Electronic spectra of **2** (top) and **3** (bottom) in  $\text{CH}_2\text{Cl}_2$  (solid lines) and after addition of two equivalents of pyridine (broken lines).

(10 ml) was added dropwise. The reaction mixture was stirred for 12 h during which time the temperature was slowly increased to 25 °C. Water (20 ml) was carefully added and a colorless precipitate, which had formed, was collected by filtration. Additional product was obtained upon separation of the liquid phases and extraction of the aqueous phase with diethylether ( $2 \times 50$  ml) and  $\text{CH}_2\text{Cl}_2$ . After drying the combined organic

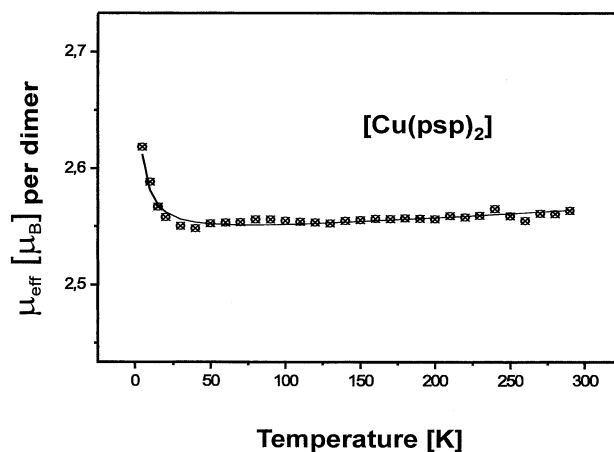


Fig. 5. Temperature-dependence of the magnetic moment,  $\mu_{\text{eff}}/\mu_{\text{B}}$ , of **1** (calculated per dimer) and best fit (solid line) using parameters given in the text.

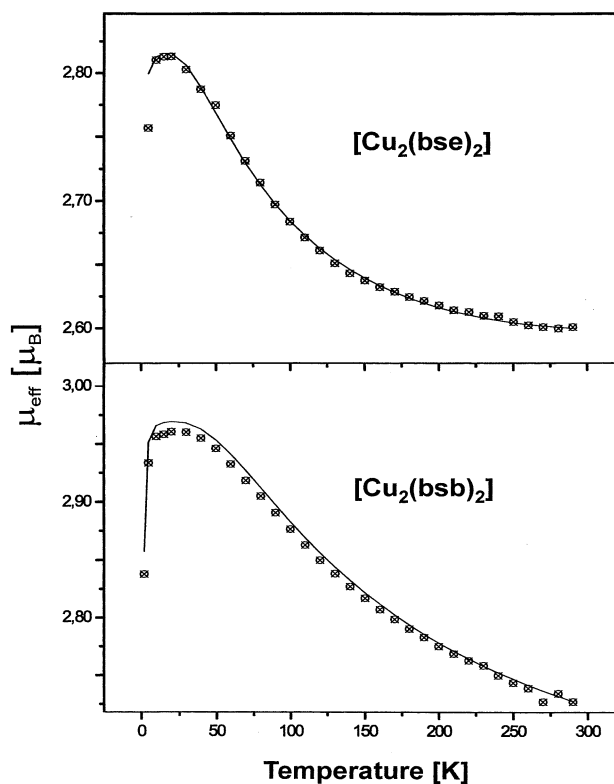


Fig. 6. Temperature-dependence of the magnetic moment/dimer of **2** (top) and **3** (bottom). The solid lines represent best fits using parameters given in the text.

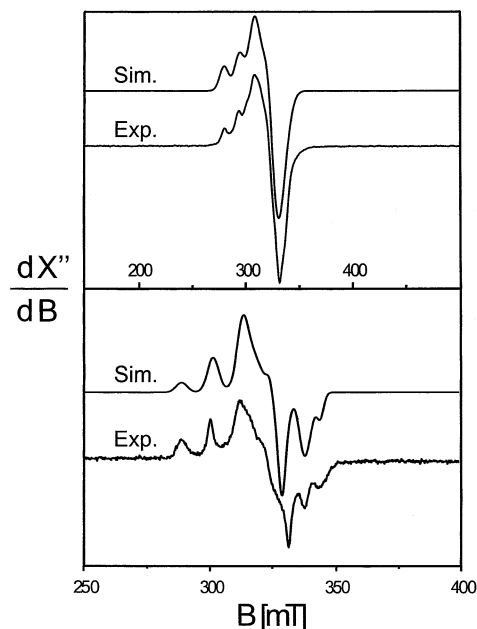


Fig. 7. X-band EPR spectra of frozen  $\text{CH}_2\text{Cl}_2$  solutions of **4** (top) and **3** at 10 K. Conditions: **4**, frequency: 9.4368 GHz; power: 10.1  $\mu\text{W}$ ; modulation 1.25 mT; **2**, frequency: 9.4365 GHz; power 100.8  $\mu\text{W}$ ; modulation 0.99 mT.

phases over  $\text{MgSO}_4$ , the solvent was removed by evaporation under reduced pressure. The product was recrystallized from *n*-pentane at  $-20\text{ }^\circ\text{C}$ . Yield: 3.62 g (72%).  $\text{C}_{30}\text{H}_{46}\text{O}_2\text{S}_2$  (502.8): *Anal.* Calc.: C, 71.66; H, 9.22; S, 12.75. Found: C, 71.9; H, 9.4; S, 12.6%. EI-mass spectrum:  $m/z = 502 [M]^+$ .  $^1\text{H}$  NMR (400 MHz;  $\text{CDCl}_3$ ):  $\delta = 1.25$  (18H, s); 1.37 (18H, s); 2.78 (4H, s); 7.03 (2H, s); 7.28 (2H, d); 7.30 (2H, d).  $^{13}\text{C}$  NMR (100 MHz,  $\text{CDCl}_3$ ):  $\delta = 29.42$ ; 31.51; 34.29; 35.20; 36.24; 117.44; 126.10; 130.30; 135.31; 142.35; 153.18.

### 3.1.2. 1,2-Bis(3,5-di-*tert*-butyl-2-hydroxyphenylsulfanyl)benzene ( $\text{H}_2\text{bsb}$ )

A solution of 1.6 M *n*-butyllithium in *n*-hexane (25 ml) was added to a solution of 2-bromo-4,6-di-*tert*-butylphenol in dry diethylether at  $-50\text{ }^\circ\text{C}$ . The immediately formed precipitate redissolved upon increasing the temperature to  $20\text{ }^\circ\text{C}$ . After stirring of this solution for 30 min and subsequent cooling to  $-65\text{ }^\circ\text{C}$ , a solution of benzene-1,2-disulfenyl dichloride (2.11 g; 10 mmol) in dry diethylether (10 ml) was added dropwise. After stirring at ambient temperature for 12 h with slow increase of the reaction temperature to  $20\text{ }^\circ\text{C}$ , a colorless precipitate formed. The following work-up was the same as described above for  $\text{H}_2\text{bse}$ . The product was recrystallized from acetone at  $-20\text{ }^\circ\text{C}$ . Yield: 3.45 g (63%).  $\text{C}_{34}\text{H}_{46}\text{O}_2\text{S}_2$  (550.9): *Anal.* Calc.: C, 74.13; H, 8.42; S, 11.64. Found: C, 75.0; H, 8.5; S, 11.4%. EI-mass spectrum:  $m/z = 550 [M]^+$ .  $^1\text{H}$  NMR (400 MHz;  $\text{CDCl}_3$ ):  $\delta = 1.30$  (18H, s); 1.40 (18H, s); 6.77 (2H, q); 6.83 (2H, s); 6.97 (2H, q); 7.41 (2H, d); 7.43 (2H, d).

$^{13}\text{C}$  NMR (100 MHz,  $\text{CDCl}_3$ ):  $\delta = 29.42$ ; 31.51; 34.42; 35.34; 115.82; 126.97; 126.99; 127.75; 130.91; 135.02; 136.03; 143.01; 153.45.

### 3.1.3. 4,6-Di-*tert*-butyl-2-phenylsulfanylphenol ( $\text{Hpsp}$ )

To a solution of 2-bromo-4,6-di-*tert*-butylphenol (5.71 g; 20 mmol) in dry diethylether (25 ml) was added a solution of 1.6 M *n*-butyllithium in *n*-hexane (25 ml) at  $-50\text{ }^\circ\text{C}$ . After stirring for 30 min and at  $20\text{ }^\circ\text{C}$  and cooling to  $-65\text{ }^\circ\text{C}$ , a solution of benzenesulfenyl chloride (2.89 g; 20 mmol) in dry diethylether was added dropwise with dropwise. The work-up was the same as described for  $\text{H}_2\text{bse}$  and  $\text{H}_2\text{bsb}$ . Distillation of the residual yellow oil at  $115\text{ }^\circ\text{C}$  and  $10^{-2}$  mbar yielded 3.40 g (54%) of  $\text{Hpsp}$ .  $\text{C}_{20}\text{H}_{26}\text{OS}$  (314.5): *Anal.* Calc.: C, 76.38; H, 8.33; S, 10.20. Found: C, 76.1; H, 8.6; S, 10.1%. EI-mass spectrum:  $m/z = 314 [M]^+$ .  $^1\text{H}$  NMR (250 MHz;  $\text{CDCl}_3$ ):  $\delta = 1.28$  (9H, s); 1.40 (9H, s); 6.83 (1H, s); 7.00–7.25 (7H, m).  $^{13}\text{C}$  NMR (63 MHz,  $\text{CDCl}_3$ ):  $\delta = 29.41$ ; 31.49; 34.36; 35.27; 115.70; 125.71; 126.30; 126.82; 129.07; 131.03; 135.73; 136.46; 142.77; 153.39.

3.1.3.1.  $[\text{Cu}^{\text{II}}(\text{psp})_2]$  (**1**). To a solution of the ligand  $\text{Hpsp}$  (0.63 g; 2.0 mmol) in dry methanol (30 ml) was added under an argon atmosphere  $\text{Cu}^{\text{I}}\text{Cl}$  (98 mg; 1.0 mmol) and 280  $\mu\text{l}$  of triethylamine. The mixture was heated to reflux for 3 h. After removal of a colorless precipitate by filtration in the presence of air, brown needle shaped crystals precipitated from the solution in the presence of air. Yield: 255 mg (37%).  $\text{C}_{40}\text{H}_{50}\text{CuO}_2\text{S}_2$  (690.5): *Anal.* Calc.: C, 69.58; H, 7.30; S, 9.29. Found: C, 69.2; H, 7.4; S, 9.5%. EI-mass spectrum:  $m/z = 689 [M]^+$ .

3.1.3.2.  $[\text{Cu}^{\text{II}}(\text{bse})_2]$  (**2**).  $\text{Cu}^{\text{I}}\text{Cl}$  (49 mg; 0.5 mmol) and 140  $\mu\text{l}$  of triethylamine were added to a solution of the ligand  $\text{H}_2\text{bse}$  (251 mg; 0.5 mmol) in dry tetrahydrofuran (25 ml). After heating to reflux for 60 min under an argon atmosphere, the solution was exposed to air and cooled to  $20\text{ }^\circ\text{C}$ . The then dark blue solution was stored at  $0\text{ }^\circ\text{C}$  for 12 h whereupon colorless crystals of  $[\text{NET}_3\text{H}]\text{Cl}$  formed, which were filtered off and discarded. Removal of the solvent by evaporation under reduced pressure yielded a green microcrystalline material, which was recrystallized from acetone. Yield: 60 mg (21%).  $\text{C}_{60}\text{H}_{88}\text{Cu}_2\text{O}_4\text{S}_4$  (1128.7): *Anal.* Calc.: C, 63.85; H, 7.86; S, 11.36. Found: C, 63.8; H, 8.0; S, 11.1%. EI-mass spectrum:  $m/z = 1128 [M]^+$ .

3.1.3.3.  $[\text{Cu}^{\text{II}}(\text{bsb})_2]$  (**3**). This complex was prepared as described above for **2** using the ligand  $\text{H}_2\text{bsb}$  as starting material. One hundred and eighty milligrams of green-brown crystals (29%) were obtained after recrystallization of the crude product from  $\text{CH}_2\text{Cl}_2$ .  $\text{C}_{68}\text{H}_{88}\text{Cu}_2\text{O}_4\text{S}_4$  (1224.8): *Anal.* Calc.: C, 66.68; H, 7.24; S, 10.47.

Found: C, 66.4; H, 7.2; S, 10.4%. EI-mass spectrum:  $m/z = 1224 [M]^+$ .

3.1.3.4.  $[Cu^{II}(bsp)(py)_2]$  (**4**). A solution of **3** (0.61 g; 0.5 mmol) and pyridine (0.08 g; 1.0 mmol) in dry  $CH_2Cl_2$  (20 ml) was allowed to stand in an open vessel for 12 h. Slow evaporation of the solvent yielded violet crystals of **4** (0.19 g; 26%).  $C_{44}H_{54}CuN_2O_2S_2$  (770.6): *Anal.* Calc.: C, 68.58; H, 7.06; S, 8.32. Found: C, 68.3; H, 7.0; S, 8.5%. EI-mass spectrum:  $m/z = 611 [M - 2py]^+$ .

### 3.2. X-ray crystallographic data collection and refinement of the structures

Colorless single crystals of  $H_2(bse)$ ,  $H_2(bsb)$ , and  $H(psp)$ , a brown crystal of **1**, green–brown crystals of **2** and **3**, and a red crystal of **4** were mounted on diffractometers equipped with a cryogenic nitrogen cold stream operating at 100 K. Graphite monochromated  $Mo K\alpha$  radiation ( $\lambda = 0.71073 \text{ \AA}$ ) was used. Crystallographic data of the compounds and diffractometer types used are listed in Table 1. Final cell constants were obtained from a least square fit of a subset of several thousand intense reflections. Diffraction data were collected taking frames at  $0.3^\circ$  (Siemens SMART) and  $0.5\text{--}1.0^\circ$  (Nonius Kappa). Data were corrected for  $L_p$ . Semi empirical absorption corrections for  $H_2(bse)$ ,  $H_2(bsb)$  were carried out with the program SADABS [9]. Intensities of **2** were corrected for absorption using the Gaussian face indexed method. The Siemens SHELXTL [10] software package (Version 5) was used for solution, refinement and artwork of the structures. All structures were solved and refined by direct methods and difference Fourier techniques. Neutral atom scattering factors incorporated in the program were used. All non-hydrogen atoms were refined anisotropically except those in disordered parts of the molecules, which were isotropically refined. Split atom models were used giving satisfactory models for the disorder; details are given in the supplementary material. Hydrogen atoms were geometrically attached and treated as riding atoms with isotropic displacement parameters.

## 4. Supplementary material

Crystallographic data for  $H_2(bse)$ ,  $H_2(bsb)$ ,  $H(psp)$ , **1**, **2**, **3**, and **4** have been deposited with the Cambridge Crystallographic Data Centre as supplementary publications no. CCDC 165316–165322. Copies of the data can be obtained free of charge on application to CCDC, 12 Union Road, Cambridge CB2 1EZ, UK (fax: +44-1223-336 033; e-mail: deposit@ccdc.cam.ac.uk or www: <http://www.ccdc.cam.ac.uk>).

## Acknowledgements

We thank the Fonds der Chemischen Industrie for financial support. Heike Schucht is thanked for skillful help with the X-ray data collections.

## References

- (a) N. Ito, S.E.V. Phillips, C. Stevens, Z.B. Orgel, M.J. McPherson, J.N. Keen, K.D.S. Yadav, P.F. Knowles, *Nature* (London) 350 (1991) 87;
- (b) N. Ito, S.E.V. Phillips, K.D.S. Yadav, P.F. Knowles, *J. Mol. Biol.* 238 (1994) 799.
- (a) M.M. Whittaker, Y.-Y. Chuang, J.W. Whittaker, *J. Am. Chem. Soc.* 115 (1993) 10029;
- (b) M.M. Whittaker, W.R. Duncan, J.W. Whittaker, *Inorg. Chem.* 35 (1996) 382;
- (c) D. Zurita, C. Scheer, J.-L. Pierre, E. Saint-Aman, *J. Chem. Soc., Dalton Trans.* (1996) 4331;
- (d) D. Zurita, I. Gautier-Luneau, S. Ménage, J.-L. Pierre, E. Saint-Aman, *J. Biol. Inorg. Chem.* 2 (1997) 46;
- (e) D. Zurita, S. Ménage, J.-L. Pierre, E. Saint-Aman, *New J. Chem.* 21 (1997) 1001;
- (f) S. Itoh, S. Takayama, R. Arakawa, A. Furuta, M. Komatsu, A. Ishida, S. Takamuku, S. Fukuzumi, *Inorg. Chem.* 36 (1997) 1407;
- (g) M.A. Halcrow, L.M.L. Chia, X. Liu, E.J.L. McInnes, L.J. Yellowlees, F.E. Mabbs, J.E. Davies, *Chem. Commun.* (1998) 2465;
- (h) M.A. Halcrow, L.M.L. Chia, X. Liu, E.J.L. McInnes, L.J. Yellowlees, F.E. Mabbs, I.J. Scowen, M. McPartlin, J.E. Davies, *J. Chem. Soc., Dalton Trans.* (1999) 1753;
- (i) J.A. Halfen, B.A. Jazdzewski, S. Mahapatra, L.M. Berreau, E.C. Wilkinson, L. Que Jr., W.B. Tolman, *J. Am. Chem. Soc.* 119 (1997) 8217.
- (a) J.W. Whittaker, in: H. Sigel, A. Sigel (Eds.), *Metalloenzymes Involving Amino Acid-Residue and Related Radicals*, vol. 30, Marcel Dekker, New York, 1994, p. 315;
- (b) G.A. Landum, C.A. Ekberg, J.W. Whittaker, *Biophys. J.* 69 (1995) 674;
- (c) M.M. Whittaker, C.A. Ekberg, J. Peterson, M.S. Sendova, E.P. Day, J.W. Whittaker, *J. Mol. Cat. B: Enzymatic* 8 (2000) 3.
- P. Chaudhuri, M. Hess, U. Flörke, K. Wieghardt, *Angew. Chem., Int. Ed.* 37 (1998) 2217.
- W.H. Mueller, M. Dines, *J. Heterocycl. Chem.* 6 (1969) 627.
- (a) S.K. Mandal, L.K. Thompson, K. Nag, J.-P. Charland, E.J. Gobe, *Can. J. Chem.* 65 (1987) 2815;
- (b) W. Mazurek, B.J. Kennedy, K.S. Murray, M.J. O'Connor, J.R. Rodgers, M.R. Snow, A.G. Wedd, P.R. Zwack, *Inorg. Chem.* 24 (1985) 3258;
- (c) J. Glerup, D.J. Hodgson, E. Pedersen, *Acta Chem. Scand.* A37 (1983) 161;
- (d) S. Kallasoe, E. Pedersen, *Acta Chem. Scand.* A36 (1982) 859;
- (e) J. Bertrand, C.E. Kirkwood, *Inorg. Chim. Acta* 6 (1972) 248;
- (f) A. Bensini, D. Gatteschi, *Inorg. Chim. Acta* 31 (1978) 11.
- (a) S. Itoh, M. Taki, S. Fukuzumi, *Coord. Chem. Rev.* 198 (2000) 3;
- (b) Y. Shimazaki, S. Huth, S. Hirota, O. Yamauchi, *Bull. Chem. Soc. Jpn.* 73 (2000) 1187.
- T. Kruse, PhD Dissertation, Ruhr Universität Bochum, 2001.
- SADABS, G.M. Sheldrick, University of Göttingen 1994.
- SHELXTL V.5, Siemens Analytical X-Ray Instruments, Inc. 1994.